Brain Stimulation 7 (2014) 900–908

Contents lists available at ScienceDirect

Brain Stimulation

journal homepage: www.brainstimjrnl.com

Transcranial Focused Ultrasound Modulates Intrinsic and Evoked EEG Dynamics

Jerel Mueller [a,b], Wynn Legon [c], Alexander Opitz [b,d], Tomokazu F. Sato [e], William J. Tyler [f,*]

[a] School of Biomedical Engineering and Sciences, Virginia Tech, Blacksburg, VA 24061, USA
[b] Virginia Tech Carilion Research Institute, Roanoke, VA 24015, USA
[c] Department of Physical Medicine and Rehabilitation, University of Minnesota, MN 55455, USA
[d] Department of Clinical Neurophysiology, Georg-August-University, Göttingen, Germany
[e] Division of Biology, California Institute of Technology, Pasadena, CA 91125, USA
[f] School of Biological and Health Systems Engineering, Arizona State University, Tempe, AZ 85287, USA

ARTICLE INFO

Article history:
Received 28 May 2014
Received in revised form
26 August 2014
Accepted 27 August 2014
Available online 27 September 2014

Keywords:
Ultrasound
Neuromodulation
Oscillations
Phase
Electroencephalography (EEG)

ABSTRACT

Background: The integration of EEG recordings and transcranial neuromodulation has provided a useful construct for noninvasively investigating the modification of human brain circuit activity. Recent evidence has demonstrated that focused ultrasound can be targeted through the human skull to affect the amplitude of somatosensory evoked potentials and its associated spectral content.
Objective/hypothesis: The present study tests whether focused ultrasound transmitted through the human skull and targeted to somatosensory cortex can affect the phase and phase rate of cortical oscillatory dynamics.
Methods: A computational model was developed to gain insight regarding the insertion behavior of ultrasound induced pressure waves in the human head. The instantaneous phase and phase rate of EEG recordings before, during, and after transmission of transcranial focused ultrasound (tFUS) to human somatosensory cortex were examined to explore its effects on phase dynamics.
Results: Computational modeling results show the skull effectively reinforces the focusing of tFUS due to curvature of material interfaces. Neurophysiological recordings show that tFUS alters the phase distribution of intrinsic brain activity for beta frequencies, but not gamma. This modulation was accompanied by a change in phase rate of both beta and gamma frequencies. Additionally, tFUS modulated phase distributions in the beta band of early sensory-evoked activity but did not affect late sensory-evoked activity, lending support to the spatial specificity of tFUS for neuromodulation. This spatial specificity was confirmed through an additional experiment where the ultrasound transducer was moved 1 cm laterally from the original cortical target.
Conclusions: Focused ultrasonic energy can alter EEG oscillatory dynamics through local mechanical perturbation of discrete cortical circuits.

Introduction

Transcranial focused ultrasound (tFUS) has been demonstrated as a feasible method for transcranial neuromodulation in humans [1]. We have previously showed tFUS can alter the amplitude of somatosensory evoked potentials with a concomitant change in tactile sensory perception. It is not clear however, what the effect of tFUS is upon oscillatory neural dynamics. The integration of electroencephalographic (EEG) recordings and transcranial neuromodulation has provided a useful, non-invasive construct for investigating the alteration of neural dynamics, including effects on EEG phase dynamics [2,3]. Oscillations in the electric potential of neuronal assemblies are the result of increases and decreases at regular intervals of the extracellular voltage of the neuronal population. The responsiveness of neurons can vary depending on whether this synchronous extracellular voltage oscillation is in a lower or higher stage (phase), and the influence of this oscillating phase on neuronal processing and cognitive function has long

Thync, Inc., provided partial support through a sponsored research agreement to Virginia Polytechnic Institute and State University Additional funding was provided through a Technological Innovation Award to WJT from the McKnight Endowment for Neuroscience and by the Virginia Tech Carilion Research Institute.
* Corresponding author. Tel.: +1 617 938 7196.
E-mail address: wtyler@asu.edu (W.J. Tyler).

1935-861X/$ – see front matter
http://dx.doi.org/10.1016/j.brs.2014.08.008

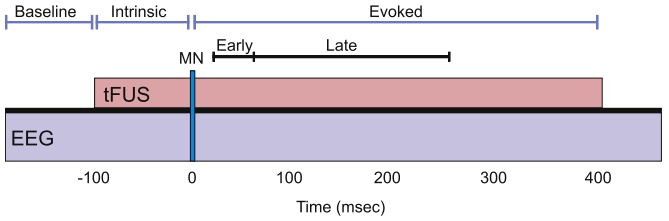

Figure 1. Schematic of the timing of events. Baseline refers to the timing of EEG before tFUS stimulation (<−100 ms). Intrinsic refers to the timing of EEG (−100 to −1 ms) during tFUS but before median nerve (MN) stimulation. Evoked refers to EEG after MN stimulation. Periods of interest include Early epoch (17–70 ms) and Late epoch (71–260 ms).

been recognized [4,5]. The application of tFUS for neuromodulation is an emerging field, and the mechanisms underlying ultrasonic neuromodulation of neural tissue are only beginning to be understood [6]. We have previously explored the effects of tFUS on the amplitude of sensory-evoked potentials and the event-related spectral content of sensory-evoked brain oscillations [1]. In the present study, we focused on investigating the feasibility and effects of tFUS on both intrinsic and evoked phase dynamics. Specifically, we were interested studying how tFUS affects both the phase and phase rate of beta and gamma oscillations that have been previously identified to be modulated by other non-invasive neuromodulation methods like transcranial magnetic stimulation [7] and transcranial alternate current stimulation [8]. Here, we report tFUS to preferentially modulate the phase of beta activity in intrinsic EEG signals but to affect both beta and gamma activity in evoked EEG responses. Lateral movement of the ultrasound transducer 1 cm from its original position ameliorated these effects, lending support for its high spatial specificity. These findings support the hypothesis that tFUS stimulation modulates EEG oscillatory dynamics similar to existing technologies and may provide a complimentary and more spatially specific form of transcranial neuromodulation.

Materials and methods

Computational modeling and acoustic field mapping

To gain insight regarding the intracranial spatial patterns and resolution of US induced pressure waves, a simple finite element method (FEM) model was constructed using COMSOL Multiphysics software (COMSOL, Inc., Burlington, MA). The modeling domain consisted of a circle ($r = 9$ cm) to approximate the brain encompassed by a 5 mm thick annulus representing the skull, and a larger annulus ($r = 15$ mm) outside the skull to provide an outer boundary of skin and acoustic coupling gel. This simple 2D geometry approximates the head as a cylinder and is valuable for developing an understanding of the basic insertion behavior of US as it propagates across model tissue layers (skin and skull) into the brain. The density (ρ) of brain was specified as 1030 kg/m^3 and the speed of sound (c) was 1550 m/s [9]. For the skull, ρ was set to 1912 kg/m^3 and c was estimated as 2300 m/s based on previous empirical observations [10]. The outermost annulus for skin and ultrasound gel was specified to have the material properties of water.

A plane wave incident pressure field of 100 Pa across a range of acoustic frequencies from 5 kHz to 2 MHz was used to represent stimulation from the US transducer. We extracted the pressure profile along a radius perpendicular to the planar acoustic waves in the FEM model to model the intracranial wavelength of US (Fig. 2A). The spatial resolution for a particular US frequency was calculated as the average distance between the peaks of the extracted pressure profiles. Assuming a linear homogenous media, the theoretical resolution can be calculated as the wavelength (λ), which is dependent on the speed of sound in the material and the wave frequency (f), by $\lambda = c/f$. The simulated wavelengths were compared to the theoretically expected wavelengths (Fig. 2B) to validate the model for visualizing the diffraction patterns of US in brain tissue (Fig. 2C).

The acoustic intensity profile of the transcranial focused ultrasound waveform was measured using a calibrated hydrophone and then projected into a realistic head FEM model as previously described [1]. Briefly, the hydrophone, US transducer, and rehydrated skull fragment were positioned in a water tank, and the position of the hydrophone manipulated using a three-axis stage and an assortment of optomechanical components. The measured tFUS acoustic field was then projected from EEG site CP3 into a three-dimensional FEM model of the head created from magnetic resonance images to estimate the acoustic field distribution in the brain during US stimulation in subjects.

Subjects

Two separate subject groups were used in experiments. The first experiment included eighteen volunteer participants (11 male, 7 female, age 18–54, mean age = 29.62 ± 10.9), which performed the experimental task with the US transducer placed at CP3. A separate sample of seven volunteer participants (5 male, 2 female, age 22–57, mean age = 28.8 ± 11.6), performed the experimental task identically with the exception that tFUS was projected from transducers placed at a site 1 cm lateral of CP3. All participants provided written informed consent to voluntarily participate in the study. None of the participants reported current drug use (prescription or otherwise) or a history of neurological impairment and all were self-report right hand dominant. Participants received remuneration for participation. The Institutional Review Board at Virginia Tech approved all procedures.

Experimental procedures

Participants were seated in a desk chair and instructed to view a cross on a computer screen in front of them. A total of 120 ultrasonic stimuli (0.5 s) were delivered at an ISI of 6 s with a positive randomization of 4 s from the 10–20 EEG site CP3. The tFUS treatment condition involved acoustically coupling the active face of the US transducer to the scalp, while the sham condition involved flipping the transducer such that the inactive face made contact with the scalp. In this manner, ultrasonic energy was not transmitted into the head and the active buzzing sound of the transducer was identical for both the sham and tFUS condition. Both sham and tFUS treatment were run in a single session counterbalanced across subjects. Total collection time was approximately 1 h. Additionally, a separate experiment with identical procedures was conducted with the transducer displaced 1 cm laterally on the scalp as a control for the spatial specificity of tFUS.

Electroencephalography (EEG) data were acquired using four 10 mm gold–silver cup electrodes placed at sites C3, CP1, CP5, and P3 referenced to the left mastoid and grounded to the left ulnar styloid process. Somatosensory evoked potentials (SEPs) were elicited in response to right median nerve stimulation delivered through a bar electrode affixed to the wrist. Amplitude was set to elicit a small but noticeable thumb twitch. In each treatment condition a total of 120 median nerve stimuli were delivered, time-locked to occur 100 ms after the onset of tFUS (Fig. 1).

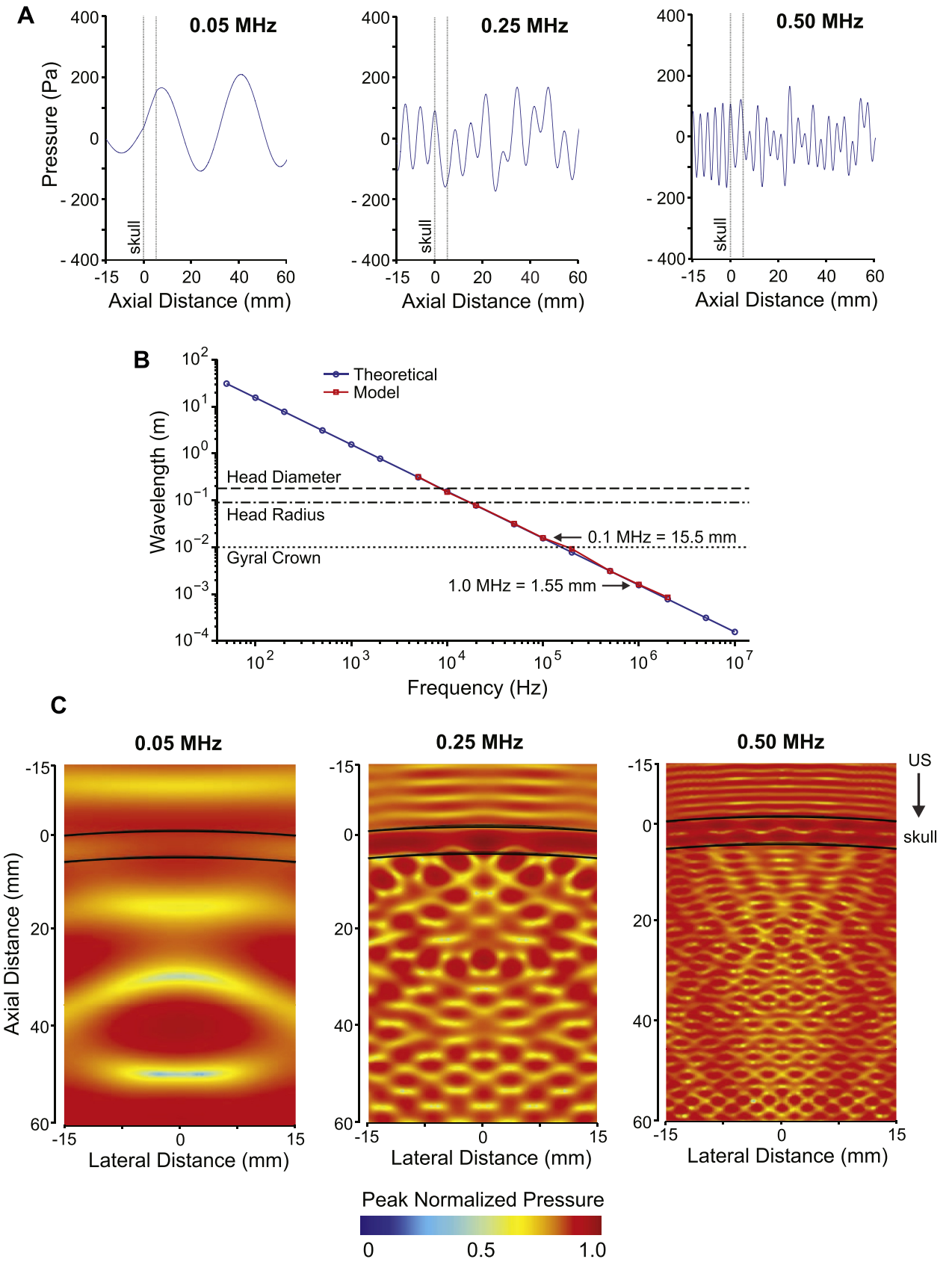

Figure 2. Model of transcranial US transmission. A, Acoustic pressure levels simulating transcranial transmission of planar ultrasound waves in the brain for the acoustic frequencies 0.05, 0.25, and 0.50 MHz. Pressure profiles within the brain region become more erratic due to interactions with neighboring pressure waves as a result of curvature of the interfaces with the skull. B, The FEM simulated and theoretical spatial resolutions of acoustic waves in the brain are plotted as a function of acoustic frequency. C, The spatial diffraction patterns of transcranial planar US modeled using FEM simulations are illustrated for the acoustic frequencies 0.05, 0.25, and 0.50 MHz.

tFUS waveform

The transcranial ultrasonic neuromodulation waveform used in these experiments has been previously described [11,12]. Briefly, transcranial ultrasonic waveforms were generated using a two-channel, 2-MHz function generator (BK Precision Instruments). Channel 1 delivered US at a pulse repetition frequency (PRF) of 1.0 kHz and channel 2 drove the transducer at a 0.5 MHz acoustic frequency (*Af*) with channel 1 serving as an external trigger for channel 2. The pulse duration (PD) of the waveform was set to 0.36 ms by adjusting the number of cycles per pulse (*c*/*p*) on channel 2–180, and the stimulus duration (0.5 s) was set by adjusting the number of pulses (np) on channel 1–500. The output of channel 2 was sent through a 40-W linear RF amplifier (E&I 240L; Electronics & Innovation) before being sent to a custom-designed focused ultrasound transducer (Blatek, Inc., State College, PA) having a center frequency of 0.5 MHz, a diameter of 30 mm and a focal length of 30 mm. The waveform employed for tFUS stimulation had the following parameters: *Af* = 0.50 MHz, PD = 360 μs, PRF = 1.0 kHz and np = 500. This produced a stimulus duration of 0.5 s yielding a peak rarefactional pressure of 0.80 MPa, a mechanical index of 1.13 and a spatial-peak pulse-average intensity (ISPPA) of 23.87 W/cm2 before transcutaneous and transcranial transmission. We have previously verified this waveform does not produce heating of the skin or skull bone. The transducer was coated with acoustic coupling gel and placed on the scalp at the 10–20 electrode location CP3 before being secured in place with athletic pre-wrap bandaging.

Data processing and calculations

All offline processing and analyses were done with Matlab v8.0 (The Mathworks, Inc., Natick, MA) using custom scripts and EEGLAB [13]. All data analyses were performed on channel CP5 as it provided the best signal to noise ratio of the electrodes. Prior to analysis, data were bandpass filtered (1–90 Hz) and notch filtered at 60 Hz using a Hamming windowed finite impulse response filter. Data were inspected for artifact and any contaminated epochs were removed from further analysis. 90 random EEG trials were used for each subject, as this was the greatest number of trials available from all subjects due to loss of data as a result of artifact rejection. Data were segmented into epochs of 2 s (−1000 ms–1000 ms) around the onset of median nerve stimulation. To avoid phase distortion, processing was done with zero-phase digital filtering using linear finite impulse response filters that had 60 dB attenuation at the specified frequency bands and a minimal filter order. Power spectra before ultrasound stimulation (−500 to −200 ms), during tFUS but before MN stimulation (intrinsic; −100 to 0 ms), and during tFUS but after MN stimulation (evoked; 1–400 ms) was calculated to ensure the EEG data had spectral content in particular frequency bands for later analyses. Power spectra were calculated by determining the fast Fourier transform of each trial, and then averaging across subjects for the time periods of interest. The shorter intrinsic time period was zero padded for increased frequency interpolation.

For each subject and each trial, phase of the EEG signal was calculated by first bandpass filtering the data with zero-phase digital filtering using linear finite impulse response filters into beta (13–30 Hz) and gamma (30–55 Hz) frequency bands. Instantaneous phase was then calculated using the Hilbert transform to first transform the real valued signal into a complex signal, whose argument then gives the instantaneous phase. Phase rate was calculated by unwrapping the instantaneous phase and calculating its slope [14]. Analyses were conducted on epochs prior to any stimulation (baseline; −200 to −100 ms), during tFUS but before MN stimulation (intrinsic; −100 to 0 ms), and during tFUS after median nerve stimulation (early and late evoked periods; Fig. 1). For the analysis of the effect of tFUS on evoked neural dynamics, two time epochs were selected after median nerve stimulation to represent early and late somatosensory activity respectively according to general timings of somatosensory early and late evoked potentials [15] such that the early epoch was specified as 17–70 ms and the later epoch was 71–260 ms. Previous literature has identified potentials up to 80 ms to be generated in primary somatosensory area [15].

Spectral content was also calculated from the trial average EEG response using the short-time Fourier transform with a window size slightly larger than the period of the average frequency of the beta (13–30 Hz, window size of 50 ms) and gamma (30–55 Hz, window size of 25 ms) frequency bands, and an overlap of half the window duration. The total power was then calculated as the sum of the spectral power within each of the time epochs of interest, calculated for each of the frequency bands separately.

Statistical analyses

The phase of EEG activity is reported to be an important consideration when delivering stimuli, as the current phase during stimulus presentation can inform us on the consequent processing of the stimuli [16]. This was not controlled during our experiments however, and prevented averaging of a subject's phase over trials, as the trial averaged phase is approximately zero due to trials not being temporally aligned by phase. Thus, to compare the instantaneous phase between stimulation conditions for each time epoch, the distributions of instantaneous phase, collected over time and trials, were tested for differences using a two-sample Kolmogorov–Smirnov test (K–S test) with Bonferroni's post hoc correction for the number of time epochs ($P < 0.0167$).

Phase rate is useful in determining differential effects on EEG dynamics independent of temporal alignment by phase. To compare the phase rate between conditions, phase rate values were averaged across each subject's trials and the distribution of mean trial values for subjects tested for significance using a two-sample Kolmogorov–Smirnov test (K–S test) with Bonferroni's post hoc correction ($P < 0.0167$). Additionally, phase rate was averaged for each subject across trials and time to obtain an average phase rate value used in a paired sample *t*-test with Bonferroni's post hoc correction ($P < 0.0167$), except for comparisons where the US transducer was displaced 1 cm laterally, which used two-sample *t*-tests, as subjects were not identical to those with the US transducer placed at CP3.

Independent of phase dynamics, differences in spectral power were assessed using the total spectral power over time of the trial averaged EEG along with a paired sample *t*-test and Bonferroni's post hoc correction ($P < 0.0167$), except for comparisons where the US transducer was displaced 1 cm laterally, which used two-sample *t*-tests, as subjects were not identical to those with the US transducer placed at CP3.

Results

Spatial resolution and diffraction patterns of transcranial ultrasound

Following distortion of the pressure waves transmitted through the model skull (located at axial distance zero), acoustic waves continued to propagate into and through the model brain having a wavelength dependent on their acoustic frequency (Fig. 2A). With increasing acoustic frequency, the wavelength of the intracranial sound pressure decreases yielding increased spatial resolutions for US, shown for our model and with a comparison to theoretical sound

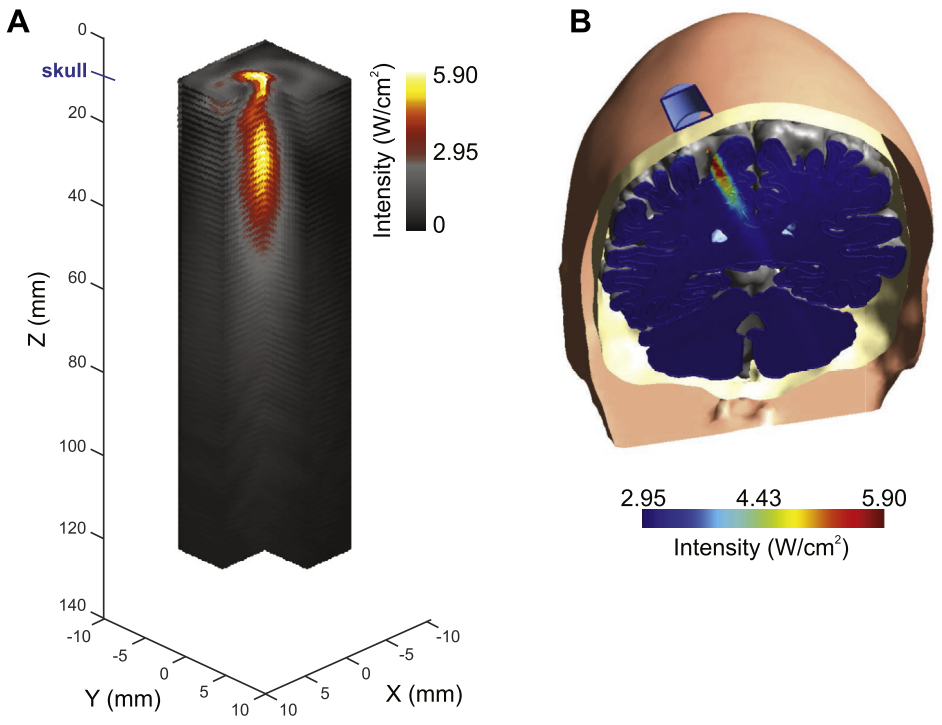

Figure 3. Transcranial transmission of focused ultrasound. A, Pseudo-color map of the acoustic intensity field emitted by the 0.5 MHz transducer after transcranial transmission through hydrated human cranial bone ($Z = 10$ mm). B, Modeled projection of the mapped acoustic intensity field from EEG scalp site CP3 into a realistic FEM model of human brain.

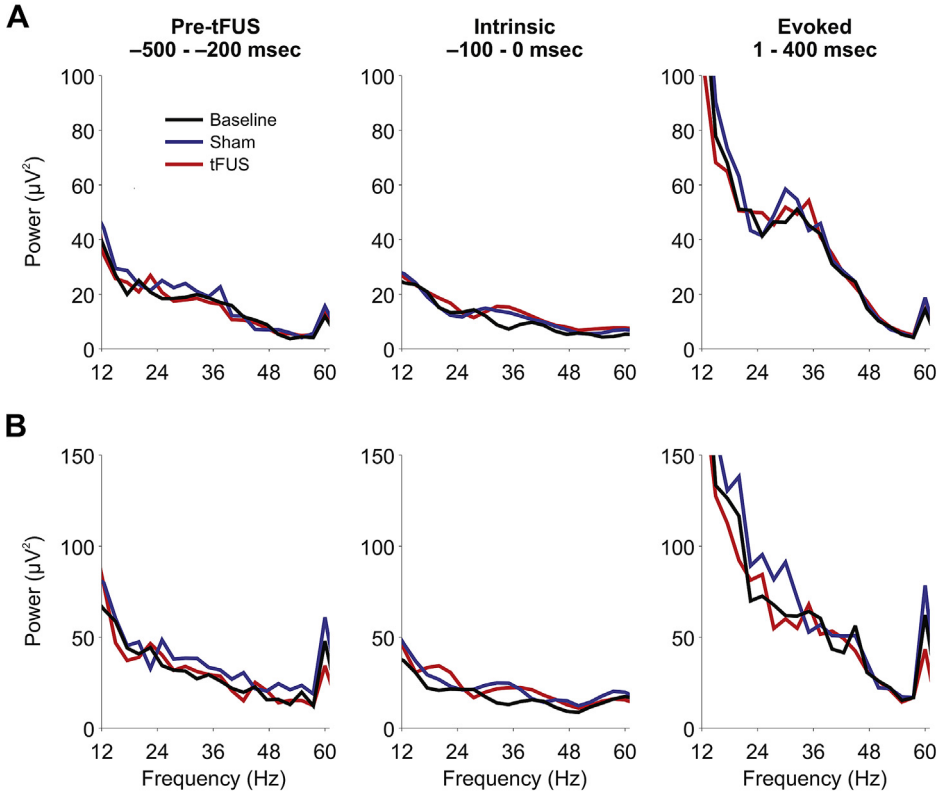

Figure 4. Power spectra of EEG data. Average power spectra recorded from electrode CP5 and calculated for the pre-tFUS, intrinsic, and evoked time periods for Sham (blue) and tFUS (red) stimulation, as well as a baseline (black) condition where subjects did not receive ultrasonic stimulation. Shown are the average power spectra for ultrasonic stimulation delivered from EEG electrode site CP3 (A, $N = 18$) and 1 cm laterally (B, $N = 7$). (For interpretation of the references to color in this figure legend, the reader is referred to the web version of this article.)

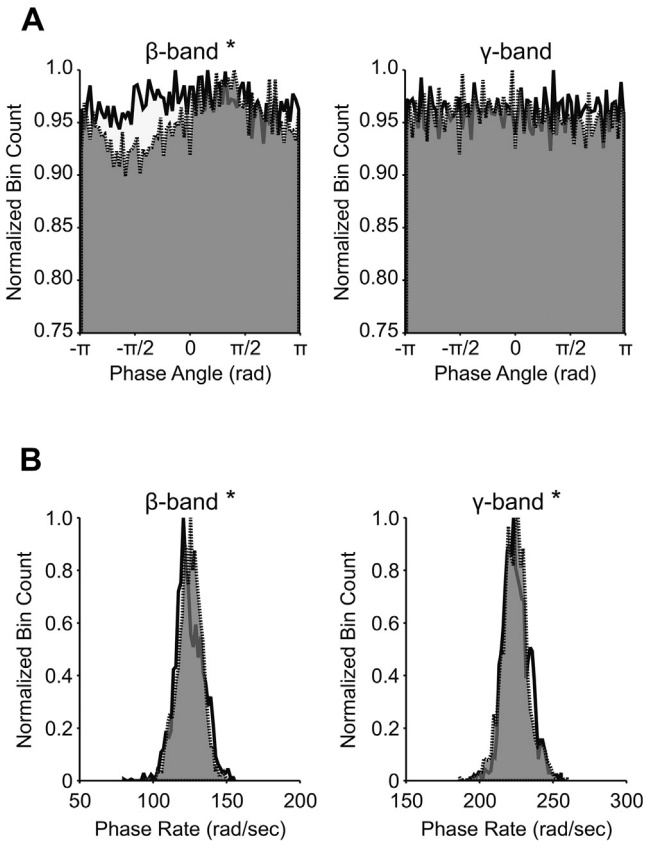

Figure 5. Effect of tFUS on baseline intrinsic EEG. Group ($N = 18$) normalized histograms of instantaneous phase (A) and phase rate (B) for the 100 msec epoch prior to MN stimulation. tFUS (white) and sham stimulation (grey) recorded at CP5 overlaid for the beta (β) and gamma (γ) frequency bands. Note the difference in profiles for the cases with significant differences. An asterisk (*) denotes a statistically significant ($P < 0.05$) difference between tFUS and sham.

pressure wavelengths in brain tissue in Fig. 2B. Additionally, due to the mismatch of material properties and curvature of material interfaces, incident sound pressure waves bend and refract as they are transmitted across the layers, producing a slight focusing effect on incident waves of planar ultrasound (US). Resultant diffraction patterns of planar US were modeled to illustrate this natural focusing effect (Fig. 2C). This focusing effect in the model held for the use of focused ultrasound as well. Transcranial mapping of the focused US transducer revealed peak intensities located about 20 mm from the face of the transducer, which drops off sharply laterally over approximately 2 mm from the center of peak effects (Fig. 3A). This profile of tFUS was found to effectively target S1 in the realistic head model in Fig. 3B when projected from site CP3 on the scalp.

Pre-stimulus baseline

The power spectra of the pre-stimulation, intrinsic, and evoked, periods are shown in Fig. 4. These results show that there was power within the frequency bands of interest (beta and gamma) recorded by the EEG for further analyses. Comparing the phase distributions during this time period, no statistically significant differences were found for both beta ($D = 3.31e{-}3$, $P = 0.33$) and gamma ($D = 2.38e{-}3$, $P = 0.74$) frequency bands. Regarding the phase rate, the trial and time averaged phase rate of subjects indicated no significant effects between tFUS and sham conditions for beta ($t(17) = -2.14$, $P = 0.047$) or gamma ($t(17) = 0.80$, $P = 0.44$). There were also no baseline differences for beta phase rate ($t(6) = 0.86$, $P = 0.42$) or gamma phase rate ($t(6) = -0.66$, $P = 0.53$) between the separate groups for the laterally displaced (1 cm) transducer. Similarly, the total spectral power indicated no effects between tFUS and sham conditions for beta ($t(17) = 0.23$, $P = 0.82$) or gamma ($t(17) = 0.37$, $P = 0.71$). There were also no differences in baseline power between the two groups for the separate groups in experiment 2; for beta ($t(6) = 0.77$, $P = 0.47$) or gamma ($t(6) = -0.07$, $P = 0.95$).

Modulation of intrinsic neural dynamics with tFUS

Phase

The distribution of instantaneous phase during the 100 ms time epoch, when tFUS was active prior to MN stimulation demonstrated a statistically significant difference between tFUS and sham stimulation for the beta frequency band ($D = 7.97e{-}3$, $P = 6.08e{-}5$) though no statistical difference in gamma phase was found ($D = 3.23e{-}3$, $P = 0.36$; Fig. 5A).

Phase rate

Phase rate provides a measure of the modulation of instantaneous phase, or phase velocity. The trial and time averaged phase rate indicated no effect between tFUS and sham stimulation for beta ($t(17) = -1.01$, $P = 0.33$) or gamma frequency ($t(17) = 0.70$, $P = 0.49$). However, statistically significant differences in phase rate distributions were found between tFUS and sham stimulation in both the beta ($D = 0.095$, $P = 1.50e{-}7$) and gamma ($D = 0.069$, $P = 3.45e{-}4$) frequency bands (Fig. 5B).

Spectral power

The total spectral power within the beta and gamma frequency bands in the 100 ms time epoch prior to MN stimulation showed no effects due to tFUS or sham stimulation (beta: $t(17) = 0.70$, $P = 0.49$; gamma: $t(17) = 0.23$, $P = 0.82$).

Effect of tFUS on evoked neural dynamics

Phase

Based upon previous results for an effect of tFUS upon the amplitude of specific potentials of the somatosensory evoked potential (SEP) [1], we examined instantaneous phase in specific time bins according to early and late SEP potential latencies. For the early SEP epoch a statistically significant difference in phase was found between tFUS and sham stimulation in the beta band ($D = 0.010$, $P = 1.92e{-}4$) but not for gamma frequency band ($D = 5.99e{-}3$, $P = 0.086$). For the late SEP epoch no statistical differences in beta ($D = 1.98e{-}3$, $P = 0.59$) or gamma phase were found ($D = 9.32e{-}4$, $P = 1.00$; Fig. 6A).

Phase rate

The trial and time averaged phase rate indicated no effect between tFUS and sham stimulation on evoked neural dynamics in the early epoch for beta ($t(17) = -0.77$, $P = 0.45$); or gamma frequencies ($t(17) = 1.15$, $P = 0.27$). There were no differences for the late epoch for both beta ($t(17) = -0.99$, $P = 0.33$) or gamma ($t(17) = 0.50$, $P = 0.62$). The analysis of phase rate distributions for the early SEP epoch found a statistical difference between tFUS and sham in the gamma band ($D = 0.090$, $P = 7.60e{-}4$) but not the beta band ($D = 0.055$, $P = 0.11$; Fig. 6B). For the late SEP epoch statistical differences were found in both the beta ($D = 0.080$, $P = 6.03e{-}10$) and gamma ($D = 0.048$, $P = 7.33e{-}4$) frequency bands (Fig. 6B). Thus, differences in phase rate were not captured by the overall mean value.

Spectral content

There were no statistically significant effects in the early SEP epoch for beta ($t(17) = 0.28$, $P = 0.78$) or gamma ($t(17) = 0.47$,

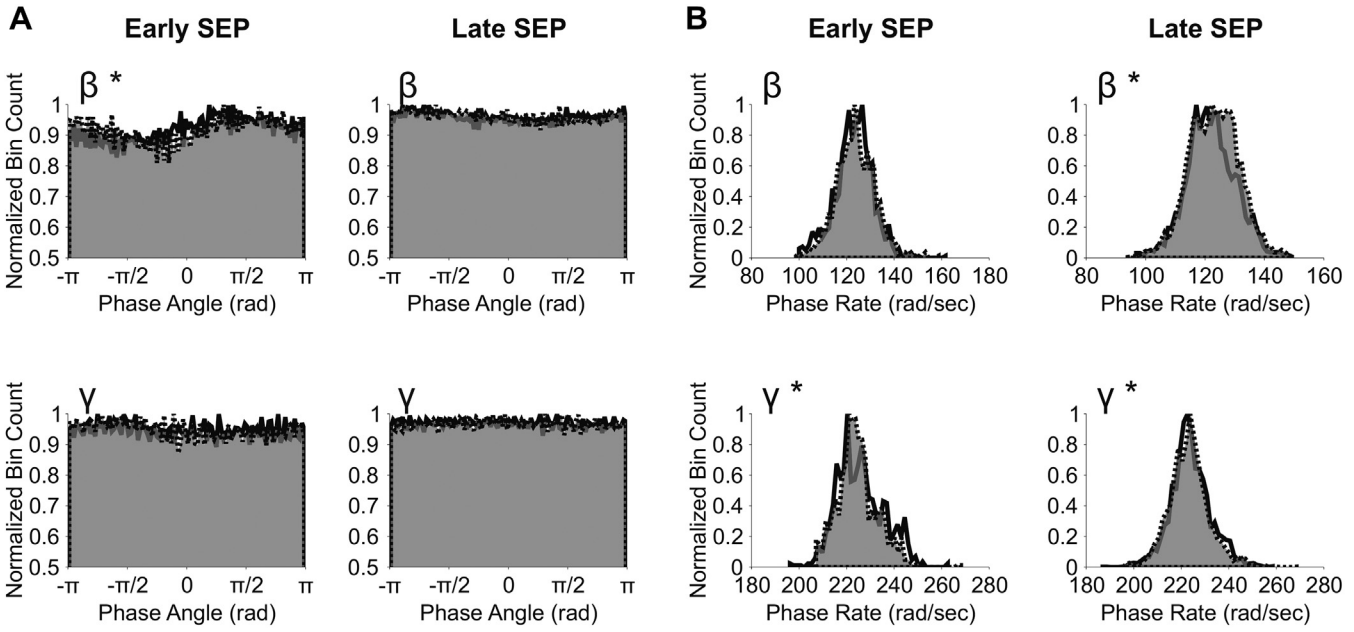

Figure 6. Effect of tFUS on evoked EEG. Normalized group ($N = 18$) histograms of evoked dynamics between tFUS (white) and sham (grey) stimulation recorded at CP5. A, Normalized histograms of instantaneous phase for the evoked early epoch and late epoch for beta (β) and gamma (γ) frequencies. B, Normalized group ($N = 18$) histograms of instantaneous phase rate for beta (β) and gamma (γ) frequencies. An asterisk (*) denotes statistical significance $P < 0.05$.

$P = 0.64$) and no statistically significant differences in the late epoch for beta ($t(17) = -0.49$, $P = 0.63$) or gamma power ($t(17) = -0.31$, $P = 0.76$).

Spatial specificity

To test the spatial specificity of tFUS effects on evoked neural dynamics, the US transducer was positioned 1 cm lateral from the original position. For the early SEP epoch statistical differences in phase distributions were found between tFUS delivered at scalp site CP3 and scalp site 1 cm lateral in the beta band ($D = 0.012$, $P = 2.56e{-3}$) but not in the gamma band ($D = 5.46e{-3}$, $P = 0.46$; Fig. 7A). For the late SEP epoch, no statistical differences were found in either the beta ($D = 3.68e{-3}$, $P = 0.19$) or gamma band ($D = 2.60e{-3}$, $P = 0.61$; Fig. 7A).

The trial and time averaged phase rate showed an effect due to placement of the US transducer in the gamma band for both the early ($t(23) = -5.00$, $P = 4.67e{-5}$) and late ($t(23) = -8.25$, $P = 2.53e{-8}$) epochs, but no effects upon the beta band for early ($t(23) = 0.25$, $P = 0.80$) or late ($t(23) = 0.12$, $P = 0.91$) epochs (Fig. 8A). Regarding phase rate distributions, the early SEP epoch did not have significant statistical differences between tFUS delivered at scalp site CP3 and scalp site 1 cm lateral in the beta band ($D = 0.065$, $P = 0.19$), but was significantly different in the gamma band ($D = 0.66$, $P = 4.49e{-104}$). For the late epoch, significant statistical differences were found in both the beta ($D = 0.071$, $P = 1.28e{-4}$) and gamma bands ($D = 0.78$, $P = 0.01$; Fig. 7B).

The total spectral power showed no effect of US transducer location in the early SEP epoch for beta ($t(23) = 0.88$, $P = 0.39$) or gamma ($t(23) = 1.02$, $P = 0.32$). There was an effect in both the beta ($t(23) = -4.50$, $P = 1.63e{-4}$) and gamma ($t(23) = -3.62$, $P = 0.0014$) frequency bands of the late SEP epoch (Fig. 8B).

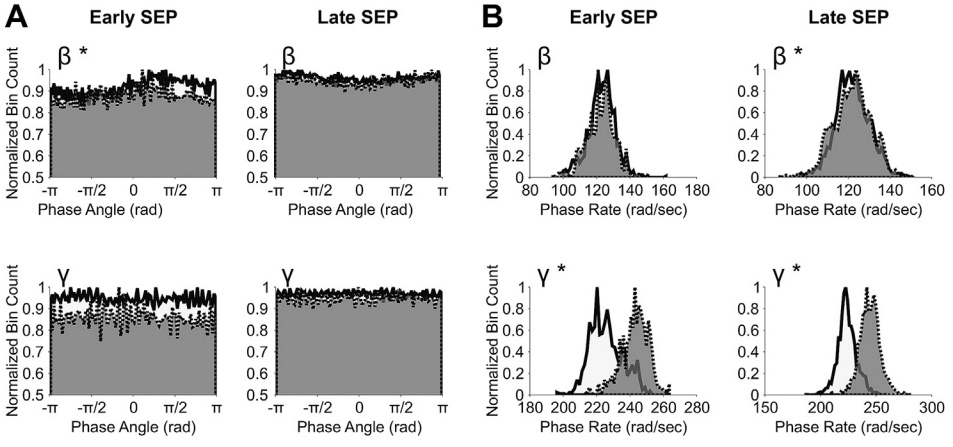

Figure 7. Effect of US transducer movement on EEG. tFUS stimulation (white, $N = 18$) and tFUS displaced 1 cm laterally (grey, $N = 7$) recorded at electrode site CP5. A, Instantaneous phase for the evoked early epoch and late epoch for beta (β) and gamma (γ) bands. B, Normalized group histograms for comparison of instantaneous phase rate for beta (β) and gamma (γ) frequencies. An asterisk (*) denotes statistical significance $P < 0.05$.

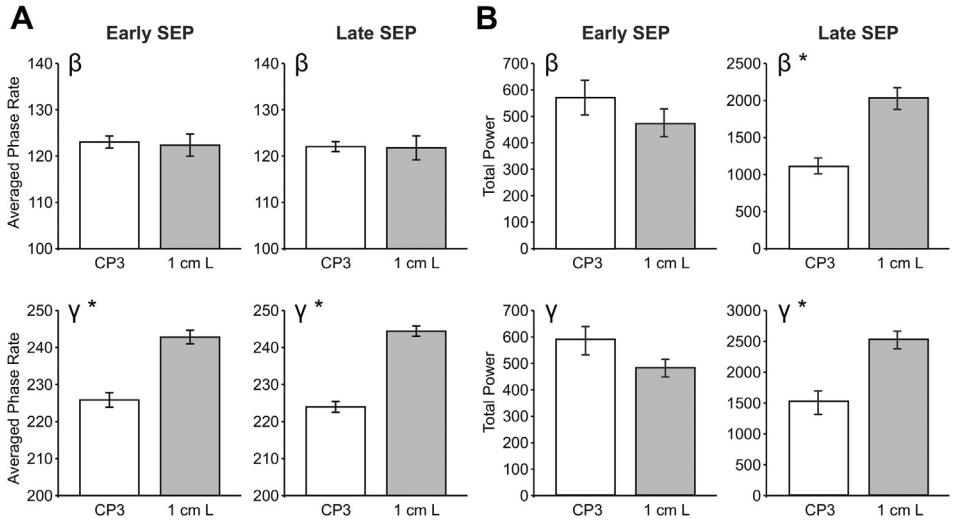

Figure 8. Effect of movement of US transducer on total spectral power. A, Group average phase rate for both the early and late evoked time bins for beta (β) and gamma (γ) frequency bands for placement of the ultrasound transducer at the original location (CP3, white, $N = 18$) and moved 1 cm laterally (1 cm L, grey, $N = 7$). B, Group average total spectral power observed following tFUS stimulation at original scalp location (CP3, white, $N = 18$) and 1 cm laterally (1 cm L, grey, $N = 7$) for beta (β) and gamma (γ) bands. An asterisk (*) denotes statistical significance $P < 0.05$.

Discussion

In this study we examined the effects of tFUS on intrinsic and evoked EEG oscillatory dynamics. Computational modeling results provided insight into the frequency dependence of intracranial pressure diffraction patterns and show the skull effectively reinforces the focusing of tFUS. Our EEG recordings show that tFUS preferentially affected the phase of beta band but not gamma-band frequencies of intrinsic brain activity. Interestingly, tFUS did modulate the phase rate of both beta and gamma intrinsic activity. We found tFUS affected phase distributions in the beta band of early sensory-evoked activity but had no effects on late sensory-evoked activity, lending support to the spatial specificity of tFUS for neuromodulation. This spatial specificity was confirmed through an additional experiment in which we moved the ultrasound transducer 1 cm laterally from the original cortical target.

Spatial resolution of tFUS

Our computational FEM model revealed the 0.5 MHz transducer used here conferred a lateral resolution of approximately 3.1 mm that is ideal for targeting specific locations within individual gyri. The models further demonstrated the skull produced dense diffraction patterns of acoustic waves, but that the skull curvature provided a slight improvement in the resolution of focal acoustic fields. These results generalize to the anatomical geometry of an actual skull as well, where the curvature would provide some additional focusing of incoming waves of focused acoustic waves specifically within the US beam focal zone. The combination of small lateral and vertical resolution using tFUS, plus controlled axial resolution, allows for neuromodulation of discrete cortical circuits superior to transcranial magnetic stimulation (TMS) for example, which produces electric fields in the cortex spanning several centimeters [17] and is presently constrained by a depth-focality trade off [18].

Neural dynamics

The phase of the ongoing intrinsic EEG has been associated with various cognitive functions [19] and the coupling or temporal synchrony is considered a critical mechanism for these functions. It is not clear in these results why acoustic energy preferentially affected the phase of beta but not gamma frequencies, but this may be due to the focus of mechanical energy preferentially affecting the resonance of pyramidal cells and/or ascending pathways in layer five that have been demonstrated to largely contribute to beta oscillations [20]. Despite this hypothesis, tFUS altered the distribution of phase rate in all time epochs and frequencies of interest. The phase of the ongoing EEG may be considered to be the oscillation of the electric potential generated by temporally aligned excitatory post-synaptic potentials from pyramidal cells of a large neural mass. The precise mechanisms underlying phase rate are not explicitly understood, however, phase rate changes may be the result of local recurrent inhibitory mechanisms that serve to keep the balance between excitation and inhibition. Indeed, there is evidence for pyramidal cell mediated activation of inhibitory cells in the rat somatosensory cortex that serve to maintain the balance between excitation and inhibition [21]. As such, changes in phase rate may represent activity of these circuits for the facilitation of signal transmission between populations with similar or resonant oscillatory phase characteristics. Within previous literature, phase rate is framed as a means of self-organization [22,23] and as a useful indicator of transitions in states. Freeman and colleagues posit that variations in phase rate is evidence that cortex is unstable in the sense that it jumps between states, yet conditionally stable in that neurons self-organize their activity, which is not readily evident in the ongoing EEG signal and in small changes in phase [22]. Inspection of the trial and time averaged phase rate may also not reflect the finer changes in oscillatory activity due to the loss of information from averaging, as reflected in our analyses of variation of phase rate indicating no effects between tFUS and sham stimulation. Phase rate was also previously implicated in cumulative changes in neural activity due to prolonged single-pulse TMS [24].

The SEP elicited by median was used to introduce coordinated temporal and spatial activity into the EEG to inspect for changes in phase dynamics localized to areas of the cortex according to evoked potential latencies [25]. We found significant differences in the instantaneous phase distributions due to tFUS in the beta frequency bands corresponding to the early and late SEP components. Furthermore, these phases were unique from those due to tFUS

when the transducer was displaced 1 cm laterally, suggesting tFUS stimulation is uniquely able to modulate the phase activity of the beta frequency band of SEP components dependent upon spatial positioning. The effect upon phase was modest and selective, while the effect of tFUS upon phase rate was rather robust across frequencies and time points, suggesting that phase rate may be a more sensitive parameter for exploring modulation in EEG phase dynamics, or that the mechanical bio-effects of tFUS are particularly effective upon the neural circuitry involved in maintaining phase but does not necessarily directly contribute to the phase of the measured signal.

Interestingly, differences in total spectral power were absent for tFUS modulation between the transducer locations during the early components of the SEP, but were present during the later time periods. We observed that tFUS modulation at the original scalp position resulted in lower total sum power than tFUS did upon moving the transducer laterally, and may be from a weaker effect on SEP neuronal activity due to stimulation being located further from S1. We find it not surprising that differences can be found in phase dynamics independent of differences in spectral information. The exact roles of spectral magnitude and phase dynamics on, for example, the generation of event-related potentials remains largely conjectured in literature, as evidenced by the continued debate between the evoked and oscillatory models of event-related potential generation [26–28]. Nevertheless, depending upon spatial location and the timing of delivery, this work adds to the recent mounting evidence [1,29–31] that focused ultrasound can be targeted to discrete cortical circuitry at spatial resolutions superior to existing non-invasive electrical and electromagnetic techniques to affect certain behaviors [1,29] in response to acute neuromodulation.

Acknowledgments

The authors would like to thank Aaron Barbour and Amanda Williams for help with data collection. WJT is a co-founder of Thync. Inc., a company developing non-invasive brain stimulation methods and devices.

References

[1] Legon W, et al. Transcranial focused ultrasound modulates the activity of primary somatosensory cortex in humans. Nat Neurosci 2014;17(2):322–9.
[2] Thut G, Miniussi C. New insights into rhythmic brain activity from TMS-EEG studies. Trends Cogn Sci 2009;13(4):182–9.
[3] Helfrich RF, et al. Entrainment of brain oscillations by transcranial alternating current stimulation. Curr Biol 2014;24(3):333–9.
[4] Basar E, et al. Gamma, alpha, delta, and theta oscillations govern cognitive processes. Int J Psychophysiol 2001;39(2–3):241–8.
[5] Engel AK, Fries P, Singer W. Dynamic predictions: oscillations and synchrony in top-down processing. Nat Rev Neurosci 2001;2(10):704–16.
[6] Tyler WJ. OPINION the mechanobiology of brain function. Nat Rev Neurosci 2012;13(12):867–78.
[7] Wozniak-Kwasniewska A, et al. Changes of oscillatory brain activity induced by repetitive transcranial magnetic stimulation of the left dorsolateral prefrontal cortex in healthy subjects. Neuroimage 2014;88:91–9.
[8] Herrmann CS, et al. Transcranial alternating current stimulation: a review of the underlying mechanisms and modulation of cognitive processes. Front Hum Neurosci 2013:7.
[9] Goss SA, Johnston RL, Dunn F. Comprehensive compilation of empirical ultrasonic properties of mammalian-tissues. J Acoust Soc Am 1978;64(2):423–57.
[10] Pichardo S, Sin VW, Hynynen K. Multi-frequency characterization of the speed of sound and attenuation coefficient for longitudinal transmission of freshly excised human skulls. Phys Med Biol 2011;56(1):219–50.
[11] Tufail Y, et al. Ultrasonic neuromodulation by brain stimulation with transcranial ultrasound. Nat Protoc 2011;6(9):1453–70.
[12] Legon W, et al. Pulsed ultrasound differentially stimulates somatosensory circuits in humans as indicated by EEG and FMRI. PLoS One 2012;7(12):e51177.
[13] Delorme A, Makeig S. EEGLAB: an open source toolbox for analysis of single-trial EEG dynamics including independent component analysis. J Neurosci Methods 2004;134(1):9–21.
[14] Freeman WJ, Rogers LJ. Fine temporal resolution of analytic phase reveals episodic synchronization by state transitions in gamma EEGs. J Neurophysiol 2002;87(2):937–45.
[15] Allison T, Mccarthy G, Wood CC. The relationship between human long-latency somatosensory evoked-potentials recorded from the cortical surface and from the scalp. Electroencephalogr Clin Neurophysiol 1992;84(4):301–14.
[16] Vanrullen R. Ongoing EEG phase as a trial-by-trial signature of perceptual and attentional rhythms. Perception 2011;40:6.
[17] Opitz A, et al. Physiological observations validate finite element models for estimating subject-specific electric field distributions induced by transcranial magnetic stimulation of the human motor cortex. Neuroimage 2013;81:253–64.
[18] Deng ZD, Lisanby SH, Peterchev AV. Electric field depth-focality tradeoff in transcranial magnetic stimulation: simulation comparison of 50 coil designs. Brain Stimul 2013;6(1):1–13.
[19] Basar E, et al. Brain oscillations in perception and memory. Int J Psychophysiol 2000;35(2–3):95–124.
[20] Lee JH, Whittington MA, Kopell NJ. Top-Down beta rhythms support selective attention via interlaminar interaction: a model. PloS Comput Biol 2013;9(8).
[21] Kapfer C, et al. Supralinear increase of recurrent inhibition during sparse activity in the somatosensory cortex. Nat Neurosci 2007;10:743Nat Neurosci. 2007;10(8):1073.
[22] Freeman WJ, et al. Fine spatiotemporal structure of phase in human intracranial EEG. Clin Neurophysiol 2006;117(6):1228–43.
[23] Freeman WJ. Origin, structure, and role of background EEG activity. Part 2. Analytic phase. Clin Neurophysiol 2004;115(9):2089–107.
[24] Stamoulis C, et al. Single pulse TMS-induced modulations of resting brain neurodynamics encoded in EEG phase. Brain Topogr 2011;24(2):105–13.
[25] Allison T, et al. Potentials-evoked in human and monkey cerebral-cortex by stimulation of the median nerve - a review of scalp and intracranial recordings. Brain 1991;114:2465–503.
[26] Klimesch W, et al. Event-related phase reorganization may explain evoked neural dynamics. Neurosci Biobehav Rev 2007;31(7):1003–16.
[27] Sauseng P, et al. Are event-related potential components generated by phase resetting of 1435 brain oscillations? A critical discussion. Neuroscience 2007;146(4):1435–44.
[28] Shah AS, et al. Neural dynamics and the fundamental mechanisms of event-related brain potentials. Cereb Cortex 2004;14(5):476–83.
[29] Deffieux T, et al. Low-intensity focused ultrasound modulates monkey visuomotor behavior. Curr Biol 2013;23(23):2430–3.
[30] Tufail Y, et al. Transcranial pulsed ultrasound stimulates intact brain circuits. Neuron 2010;66(5):681–94.
[31] Yoo SS, et al. Focused ultrasound modulates region-specific brain activity. Neuroimage 2011;56(3):1267–75.